# On lower order strain gradient plasticity theories

## Christian F. Niordson [a,*], John W. Hutchinson [b]

[a] *Department of Mechanical Engineering, Technical University of Denmark, DK-2800 Kgs. Lyngby, Denmark*
[b] *Division of Engineering and Applied Sciences, Harvard University, Cambridge, MA 02138, USA*

## Abstract

By way of numerical examples, this paper explores the nature of solutions to a class of strain gradient plasticity theories that employ conventional stresses, equilibrium equations and boundary conditions. Strain gradients come into play in these modified conventional theories only to alter the tangent moduli governing increments of stress and strain. It is shown that the modification is far from benign from a mathematical standpoint, changing the qualitative character of solutions and leading to a new type of localization that is at odds with what is expected from a strain gradient theory. The findings raise questions about the physical acceptability of this class of strain gradient theories.
© 2003 Éditions scientifiques et médicales Elsevier SAS. All rights reserved.

*Keywords:* Strain gradient plasticity; Non-local mechanics

## 1. Introduction

Conventional continuum theories of plasticity have no constitutive length scale. Any size-dependence in the relationship between load and deformation depends entirely on geometric dimensions. There is now ample experimental evidence that geometric dimensions alone cannot account for observed size-dependence of the plastic response of micron-sized solid objects. Typically, at a scale below tens of microns, but depending on object shape and the type of loading, departures are observed which can only be interpreted within the confines of conventional theory as an apparent increase in flow strength. It is generally accepted that this apparent increase in flow strength is due to the generation of geometrically necessary dislocations that accompany non-uniform plastic straining. It is argued that micron-scale gradients produce geometrically necessary dislocations at a density comparable to that of statistically stored dislocations, thereby increasing the total dislocation density and the resistance to plastic flow.

Continuum theories have been proposed recently to extend the validity of conventional plasticity down to roughly the micron scale. For a continuum theory to have validity, the number of dislocations within a typical representative volume element must be sufficiently large such that meaningful averages over the dislocations can be taken, at least in principle. Based on experimental observation of load-deformation responses, the apparent range of applicability of a continuum plasticity theory in most instances appears likely to extend upward from the micron, or possibly sub-micron, scale. The limit of any such theory when the length characterizing the deformation field becomes large compared to the constitutive length parameters should be the corresponding conventional theory. Continuum strain gradient plasticity theories have been proposed for single crystals (e.g., Gurtin, 2000; Arsenlis and Parks, 1999; Busso et al., 2000) and as extensions of the classical phenomenological theories of plasticity (e.g., de Borst and Mühlhaus, 1992; Gao et al., 1999; Bassani, 2001; Fleck and Hutchinson, 2001). These theories divide into two classes: those with conventional stresses, equilibrium equations and boundary conditions (e.g., Bassani, 2001; Arsenlis and Parks, 1999; Busso et al., 2000); and those having additional stress quantities and additional boundary conditions (e.g., de Borst

---

and Mühlhaus, 1992; Gao et al., 1999; Gurtin, 2000; Fleck and Hutchinson, 2001). For want of a better terminology, a member of the former class is referred to here as a lower order strain gradient theory, while a member of the latter is termed a higher order gradient theory.

Lower order gradient theories are addressed in the present paper. These theories are intrinsically incremental in nature with stresses, incremental equilibrium equations and boundary conditions that are taken to be the same as in conventional theory. Only the incremental constitutive relation is different from conventional theory. In the rate-independent version of these theories, which will be considered here, the constitutive relation is altered by incorporating a dependence on the gradient of plastic strain in the tangent moduli, reflecting the increased flow resistance.

In the course of carrying out a numerical analysis of a basic boundary value problem with one particular version of the lower order gradient theories, it was noticed that some seemingly anomalous behavior emerged in the form of an inexplicable localization of flow. This lead us to step back and analyze several elementary problems with the aim of more clearly revealing the nature of solutions to this class of theories. For the two problems explored here, it will be seen that solutions with an unusual form of localization occurs that appears to be unphysical in nature. Contrary to a smoothing of steep gradients that is expected to follow from the introduction of a gradient theory, the lower order gradient theory promotes the development of certain kinds of discontinuities. These findings raise issues as to the soundness of this class of theories, which are discussed at the conclusion of the paper.

## 2. A lower order strain gradient theory

A generalization of $J_2$-flow theory proposed by Acharya and Bassani (1996) and Bassani (2001) to account for size effects due to hardening by plastic strain gradients is employed here. This lower order isotropic hardening theory represents the most direct and simplest generalization of classical theory that incorporates size-dependence associated with a material length parameter. The version of the formulation introduced below assumes small strains and small rotations. The strain-displacement relation is the conventional one, $\varepsilon_{ij} = \frac{1}{2}(u_{i,j} + u_{j,i})$, as are the stresses, $\sigma_{ij} = \sigma_{ji}$, and the incremental equations of equilibrium, $\dot{\sigma}_{ij,j} = 0$ (no body forces). Plastic strain gradients are introduced through a positive invariant, $\alpha$, of the gradient of the plastic strain tensor $\varepsilon_{ij}^p$ defined below. The constitutive relations are defined by (see Bassani, 2001)

$$\tau_e = \sqrt{\frac{1}{2} s_{ij} s_{ij}}, \tag{1}$$

$$\dot{\tau}_e = h(\gamma_e^p, l\alpha) \dot{\gamma}_e^p, \tag{2}$$

$$\dot{\varepsilon}_{ij}^p = \left(\frac{\dot{\gamma}_e^p}{2\tau_e}\right) s_{ij}, \tag{3}$$

$$\dot{\sigma}_{ij} = C_{ijkl}(\dot{\varepsilon}_{kl} - \dot{\varepsilon}_{kl}^p), \tag{4}$$

where $s_{ij}$ is the stress deviator and $\tau_e$ is the effective shear stress. The effective plastic strain, $\gamma_e^p = \int \sqrt{2\dot{\varepsilon}_{ij}^p \dot{\varepsilon}_{ij}^p}$, is work conjugate to $\tau_e$. The isotropic elastic stiffness tensor is $C_{ijkl}$. The effect of plastic strain gradients are included through Eq. (2), where it is noted that the incremental hardening modulus, $h$, depends on the plastic strain gradient measure, $\alpha$, in addition to the effective plastic strain $\gamma_e^p$. The material length parameter $l$ must be included for dimensional consistency. The specific definition of $\alpha$ used in the present work is $\alpha^2 = 2\alpha_{ij}\alpha_{ij}$ where $\alpha_{ij} = e_{jkl}\varepsilon_{il,k}^p$. The expression for $h$ is taken from Bassani (2001), and can be written as

$$h(\gamma_e^p, l\alpha) = \frac{G}{n} \left(\frac{\gamma_e^p}{\gamma_0} + 1\right)^{1/n-1} \left[1 + \frac{(l\alpha/\gamma_0)^2}{1 + c(\gamma_e^p/\gamma_0)^2}\right]^{1/2}, \tag{5}$$

where $G$ is the elastic shear modulus, $\gamma_0$ is the initial yield strain in shear, and $c$ is an adjustable parameter taken to be unity in the present work. In the limit when the combination $l\alpha/\gamma_0$ is small, $h$ reduces to classical $J_2$ flow theory with a commonly used strain hardening relation. Under uniform shearing, $\gamma_e^p/\gamma_0 \approx (\tau_e/\tau_0)^n$ as the stress becomes large, with $\tau_0 = G\gamma_0$ as the initial yield stress in shear. The role of the gradient of plastic strain in (5) is to increase the incremental hardening modulus. It should be emphasized that the specific form (5) is not critical to our discussion or qualitative findings, as will be discussed later.

## 3. Shear of an infinite layer

Consider an infinitely long elastic–plastic layer of the material of Section 2 of thickness $2D$ bonded to two rigid platens whose surfaces coincide with $x_1 = -D$ and $x_1 = D$, as in Fig. 1 with $L = \infty$. The platens are displaced parallel to one
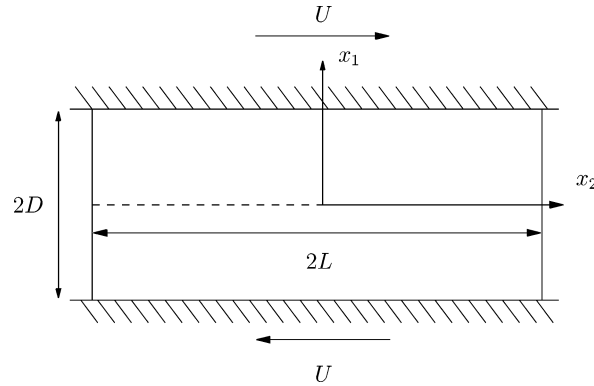
Fig. 1. A slab of material between rigid platens is analyzed under shear deformation. The elastic–plastic solid occupies the region $-L \leqslant x_2 \leqslant L$ and $-D \leqslant x_1 \leqslant D$, and the platens are displaced the distance $2U$ relative to each other in the direction of the $x_2$-axis.

another according to $u_2 = U$ on $x_1 = D$ and $u_2 = -U$ on $x_1 = -D$ imposing an average shear strain $\bar{\gamma} = 2\bar{\varepsilon}_{12} = U/D$ on the layer. In the absence of any initial non-uniformity the layer will undergo a uniform shear strain with uniform plastic strain across the layer and no gradient of plastic strain. The conventional solution satisfies the field equations even if $\ell$ is non-zero. To activate gradient effects, one must consider some initial non-uniformity. For this purpose, the layer is assumed to have an initial parabolic distribution of plastic strain across the width of the solid with $\gamma^{p(i)}(x_1) = \gamma^{(i)}(1 - (x_1/D)^2)$. This can be regarded as a pre-existing, non-uniform dislocation density across the width of the layer with $\gamma^{(i)} \geqslant 0$ being the magnitude of the initial plastic strain profile.

When the platens are displaced, the layer undergoes non-uniform shearing where the total strain, $\gamma \equiv 2\varepsilon_{12}$, elastic strain, $\gamma^e = \tau/G$ ($\tau \equiv \sigma_{12}$), and plastic strain, $\gamma^p = \gamma - \gamma^e$, depend only on $x_1$. One can readily show that the problem for the plastic strain reduces to solving the equation $\dot{\tau} = h(\gamma^p, l|\gamma^p_{,1}|)\dot{\gamma}^p$ where $\gamma^p_{,1}$ is the derivative of the plastic shear strain. Equilibrium dictates that the shear stress, $\tau$, is uniform throughout the layer, and hence so is the elastic shear strain, $\gamma^e$.

Two distributions of the initial yield stress, $\tau_Y$, will be considered, although it will be seen that the choice has little effect on the essential outcome. The simplest choice is a uniform distribution, $\tau_Y = \tau_0 = G\gamma_0$, taking no account of the initial plastic strain on initial yield. The other choice accounts for an increase in the initial yield stress due to the initial dislocation density through the hardness function. The material is assumed to have reached the initial distribution of plastic strain proportionally such that initial distribution of plastic strain evolves according to $\gamma^p(x_1) = t\gamma^{p(i)}(x_1)$ with $t$ being a parameter increasing from zero to unity. Using this assumption the initial yield stress, $\tau_y(x_1)$, can be obtained by integrating the relation $\dot{\tau}_y(x_1) = h(\gamma^p, l|\gamma^p_{,1}|)\gamma^{p(i)}(x_1)\dot{t}$.

Attention will be limited to initial distributions and solutions that are symmetric with respect to the mid-plane of the layer. Numerical solutions are obtained through a finite-difference approach, where the half width of the layer, from $x_1 = 0$ to $x_1 = D$, is modeled and discretized into 81 nodes. Load integration is performed using a Forward Euler method with load increments equal to $10^{-5}\tau_0$. A central difference scheme is employed throughout the inner nodes to evaluate the gradient of the plastic strain. Skew differences, also of second order accuracy, are employed at $x_1 = 0$ and $x_1 = D$. The skew difference at $x_1 = 0$ has the effect of allowing for a non-smooth development of the plastic strain distribution at this point, which is indeed necessary to obtain the correct solution for the problem.

The overall shear stress versus shear strain response is shown in Fig. 2 for the amplitude of the initial plastic strain distribution given by $\gamma^{(i)} = \gamma_0 = \tau_0/G$ and the associated non-uniform initial yield stress distribution. The curves in the figure correspond to different values of the material length scale $l$, with $n = 5$. As expected, an increase in $l$ gives an increase in the predicted overall stress–strain response. For the curve corresponding to $l = 0$, profiles of plastic shear strain for $x_1$ between 0 and $D$ are shown for different values of the overall shear strain in Fig. 3. Since the initial yield stress and the plastic strain are exactly matched, a constant level of plastic strain develops, and for overall strains above $\bar{\gamma}/\gamma_0 = 1.5$ the plastic strain profile is constant across the entire layer. Before yield occurs across the layer, the derivative of the plastic strain has a discontinuity at the current elastic–plastic boundary. For materials with $l > 0$ this presents a problem for the finite difference scheme. To circumvent this problem, the derivative of the plastic strain is interpolated between values of the derivative at a distance of $l/40$ on each side of the elastic–plastic boundary. Specifically, if the coordinate of the current elastic–plastic boundary is denoted $x_p$, the gradient of plastic strain is interpolated linearly between the values of the gradient at $x_1 = x_p - l/40$ and that at $x_1 = x_p + l/40$, for nodes within the interval $[x_p - l/40; x_p + l/40]$.

In Figs. 4(a) and 4(b) profiles of the plastic shear strain are shown for various levels of overall deformation, $\bar{\gamma}/\gamma_0$, when the internal material length scale is $l/D = 3$. The solid curves correspond to a material where the initial yield stress has been
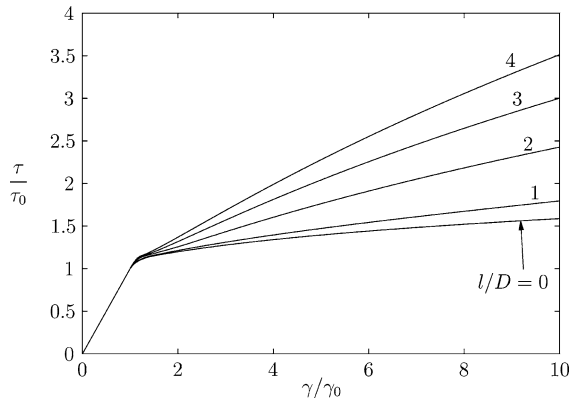
Fig. 2. Shear stress as a function of shear strain, for different values of the internal material length scale, and $L/D = \infty$.
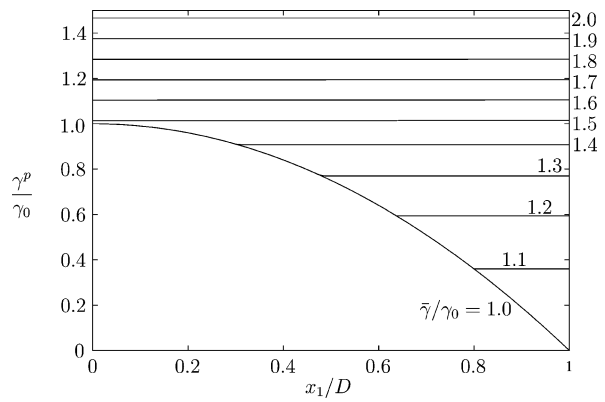
Fig. 3. Development of the plastic strain profile for a conventional material, with an initial imperfection of plastic strain, and $L/D = \infty$.
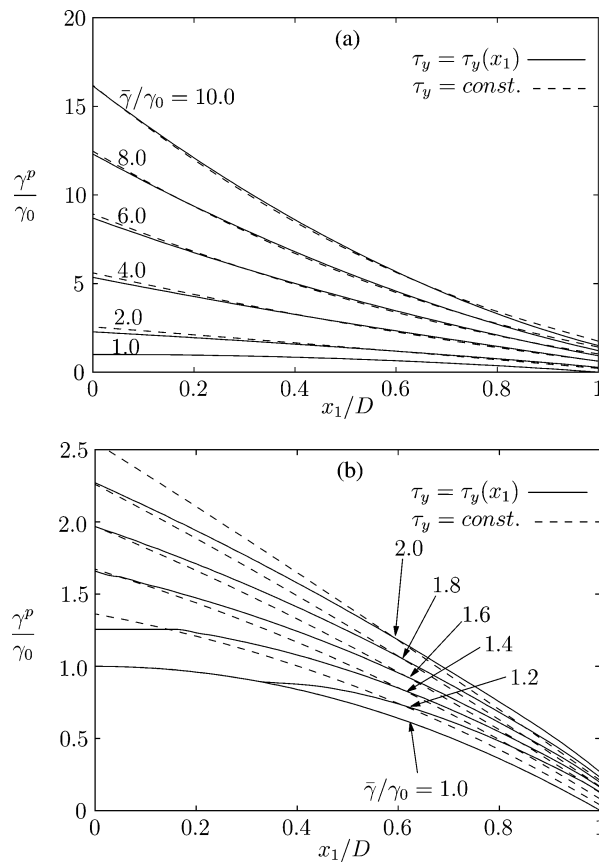


Fig. 4. The development of the profiles of effective plastic strain, along the $x_1$-axis, for an infinite slab of material ($L/D = \infty$) with an initial distribution of plastic strain, and an internal material length scale given by $l/D = 3$. The solid curves show results for a material where the initial yield stress distribution is matched to the initial plastic strain distribution, while the dashed curves show results for a material with a constant yield stress, $\tau_y = \tau_0$, which is independent of the initial plastic strain profile. In figure (a) the profiles of plastic strain are shown for an overall deformation level of up to $\bar{\gamma}/\gamma_0 = 10$, and in figure (b) the profiles are shown for an overall deformation level of up to $\bar{\gamma}/\gamma_0 = 2$.

matched to the initial level of plastic strain as described earlier, while the dashed curves show results for a material where the initial yield stress is assumed to be constant and equal to $\tau_0$. The lower curve in each of these figures shows the initial plastic strain profile corresponding to loading below initial yield, while the curves above correspond to an overall shear strain that

gives rise to additional plastic straining. The difference between the plastic strain distributions for the two choices of initial yield stress at relatively small levels of overall plastic strain is due to the way plastic yielding spreads across the layer. However, the difference becomes insignificant as the overall shear increases.

The essential feature of the solution that emerges in Fig. 4 is the development of a vertex in the plastic strain distribution corresponding to a discontinuous derivative of the plastic strain at the center of the layer at $x_1 = 0$. This unusual form of shear localization is unexpected because the incorporation of strain gradients is generally expected to smooth plastic strain distributions. Indeed, the first introduction of a gradient theory of plasticity by Aifantis (1984) was for the purpose of smoothing abrupt shear locations leading to finite width shear bands. It has become common practice to employ strain gradient dependence as a localization limiter in the analysis of materials prone to localization (e.g., Jirasek and Bazant, 2002). *By contrast, the lower order strain gradient theory appears to promote an unusual form of localization.* The occurrence of the plastic strain vertex in the present context is particularly troubling from a physical standpoint because the conventional solution to the shearing problem with $\ell = 0$ is perfectly smooth. Shear localization is excluded in the small strain formulation for a conventional hardening material ($h > 0$).

The shear problem is sufficiently simple that the reason for the development of the vertex localization is transparent. Consider the equation governing the plastic strain, $\dot{\tau} = h(\gamma^p, l|\gamma_{,1}^p|)\dot{\gamma}^p$. In the lower order gradient theory, for fixed $\gamma^p$, $h$ is necessarily a minimum with respect to $\gamma_{,1}^p$ at $\gamma_{,1}^p = 0$, since it is essential to this class of theories that gradients increase the tangent modulus. This is the case in (5). Moreover, for fixed $\gamma_{,1}^p$, $h$ decreases with increasing $\gamma^p$. It follows that any smooth distribution of $h$ with a local maximum in $\gamma^p$ will have the lowest tangent modulus at the maximum. Because $\dot{\tau}$ is uniform, it follows that $\dot{\gamma}^p$ must also be maximum at that point. Moreover, if $\gamma_{,1}^p = 0$ were to be maintained at this point, the plastic strain in the vicinity of that point would "run away" because $h$ decreases most rapidly at this point. Instead, as seen in Fig. 4, a vertex in the distribution of plastic strain develops at the point with a discontinuity in $\gamma_{,1}^p$. When $\ell \neq 0$, the combined roles of $\gamma^p$ and $\gamma_{,1}^p$ allow the balance required for satisfaction of a constant value of $\dot{\tau} = h(\gamma^p, l|\gamma_{,1}^p|)\dot{\gamma}^p$ to be achieved at the mid-point. The above argument is quite general suggesting that any hardening relation proposed for this class of lower order theories would lead to vertex-type localizations given an initial non-uniformity with a region that is locally hard.

The same qualitative reasoning can be applied to a situation where the plastic strain distribution begins with a smooth minimum such that the material is locally soft at the mid-point. Now, in the absence of any effect of $\gamma_{,1}^p$, $h$ would have a maximum at the point and $\dot{\gamma}^p$ a minimum. However, the two contributions to the tangent modulus, from both $\dot{\gamma}^p$ and $\gamma_{,1}^p$, no longer both conspire to depress $\dot{\gamma}^p$ at the mid-point. Now, they work to opposite effect. Numerical calculations similar to those described above with $\gamma^{p(i)}(x_1) = \gamma^{(i)}(x_1/D)^2$ indeed revealed that no vertex development occurs at $x_1 = 0$ if the initial plastic strain distribution has a smooth minimum at the mid-point.

The existence of solutions to the lower order theory such as those in Fig. 4 is related to the findings reported by Volokh and Hutchinson (2002) on a similar infinite layer problem in the absence of any initial non-uniformity. These authors have shown that the solution to the lower order formulation for the elementary shear problem is not unique for a material with continuous tangent modulus at the onset of yield. They produced a family of solutions, including members that are similar to those that emerge in Fig. 4. The existence of multiple solutions to the lower order theory arises from the fact that higher order terms have been introduced into the theory without an increase in the number of boundary conditions. In any problem, such as the shear problem, where initial yield occurs simultaneously over all or part of the body and where the tangent modulus is continuous at yield, the emergence of the gradient of plastic strain at the onset of yielding is indeterminate. The initial tangent modulus is also indeterminate. Multiple solutions are possible depending on how the initial gradient is specified. In the shear problem, it is possible to specify the initial gradient by requiring that an extra boundary condition be satisfied. Alternatively, an initial non-uniformity has the effect of "selecting" one of the many possible solutions. Although we have not attempted to do so, it would be interesting to conduct a systematic study to relate the initial imperfection to solution selection.

Finally, it should be mentioned that a well-formulated higher order gradient theory of plasticity does not admit multiple solutions to problems like the shear problem, nor does it lead to localization. If constraints to plastic flow at the interface with the platens are not imposed, these theories predict uniform shearing across the layer as in the case of the conventional solution. However, if the additional boundary conditions associated with the theory are used to impose constraints at the platens, non-uniform plastic flow results. For example, Fleck and Hutchinson (2001) and Bittencourt et al. (2003) model blocked dislocations at an interface by an additional boundary condition requiring the plastic strain to vanish at the platens. Even if the layer is initially uniform, non-uniform plastic deformation develops due to the boundary constraint.

## 4. Shear of a finite layer

In the problem analyzed thus far, strain gradients are triggered by an initial non-uniformity. For problems where conventional theory predicts an inhomogeneous plastic strain distribution, due to object shape or to spatial variation of the applied loads,

gradients of plastic strain develop naturally. For these problems, gradient effects will be predicted by both classes of gradient theories. A problem of this type will be studied in this section.

A finite slab of elastic–plastic material between to rigid platens is considered as depicted in Fig. 1. The slab has the thickness $2D$ and the length $2L$, and it occupies the region $-D \leqslant x_1 \leqslant D$ and $-L \leqslant x_2 \leqslant L$. As before, at $x_1 = \pm D$ displacements $u_2 = \pm U$, respectively, are prescribed with no displacement in the other two directions. The ends of the elastic–plastic slab at $x_2 = \pm L$ are traction free. Now, the requirement $\sigma_{12} = 0$ on the ends results in distinctly non-uniform behavior. Initial non-uniformity is not considered. The problem has a plane strain solution. Let $\sigma_e = \sqrt{3}\tau_e$ and $\varepsilon_e^p = (1/\sqrt{3})\gamma_e^p$. Replace (2) by

$$\dot{\sigma}_e = h\big(\varepsilon_e^p, l\alpha\big)\dot{\varepsilon}_e^p, \tag{6}$$

where instead of (5), let

$$h\big(\varepsilon_e^p, l\alpha\big) = \frac{E}{n}\left(\frac{\varepsilon_e^p}{\varepsilon_0} + 1\right)^{1/n-1}\left[1 + \frac{(l\alpha/(\sqrt{3}\varepsilon_0))^2}{1 + c(\varepsilon_e^p/\varepsilon_0)^2}\right]^{1/2}. \tag{7}$$

Now, $E$ is Young's modulus, $\nu$ is Poisson's ratio, $\varepsilon_0 = \sigma_y/E$ is the uniaxial yield strain, and $\sigma_y$ is the initial yield stress in uniaxial tension. (There is a slight difference from the constitutive relation in the last section, but they coincide for $\nu = 1/2$.)

Numerical solutions are obtained by use of the Finite Element Method with quadrilateral elements each subdivided into 4 linear displacement triangles. The gradient of the plastic strain tensor is found by assigning nodal values of the plastic strain tensor as the average of the plastic strain tensors in the elements connected to a node. Then, the gradient is evaluated for each quadrilateral at the center point by interpolating the components of the plastic strain tensors from the four nodal values of the quadrilateral using bilinear shape functions. This procedure rests on the assumption that the plastic strain field is smooth. As shown in the previous section, this will not necessarily be true for the gradient dependent solids, even though the initial plastic strain field is smooth. Load integration is performed using the Forward Euler method.

A slab of material with aspect ratio $L/D = 1$ is analyzed. The material parameters are $\varepsilon_0 = 0.01$, $\nu = 0.3$ and $n = 5$. This problem corresponds to the shear problem analyzed by Niordson and Hutchinson (2003), within the framework of the higher order strain gradient plasticity theory proposed by Fleck and Hutchinson (2001). In Fig. 5 the normalized average traction, $\bar{\tau}/\sigma_y$, as computed from the lower order gradient theory under consideration here is shown as a function of $\bar{\gamma} = U/(D\varepsilon_0)$ for different values of the internal material length scale. The figure illustrates the predicted strengthening effect due to plastic strain gradients. For $l/D = 0.25$ an increase in the average traction of around 7% relative to the conventional response is found at the overall deformation $U/(D\varepsilon_0) = 20$, while for $l/D = 0.5$ the increase is approximately 16%. These results are obtained using 20 times 20 quadratic quadrilaterals covering one fourth of the slab, enabled by the double symmetry of the problem.

In Fig. 6 the development of the effective plastic strain profile along the $x_1$-axis is shown. In each sub-figure the profile of the effective plastic strain, $\varepsilon_e^p$, is shown for five overall deformation levels; $U/(D\varepsilon_0) = 4, 8, 12, 16,$ and $20$. Each row of sub-figures shows results for different mesh refinements; the first row shows results for 10 times 10 elements covering one fourth of the slab, and the second and third row show results for 20 times 20 and 40 times 40 elements, respectively. Each column shows the development of the effective plastic strain profile for a different value of the internal material length scale normalized with respect to the half width of the slab. The first column shows the conventional predictions, while the second and third column show results for $l/D = 0.25$ and $l/D = 0.5$, respectively. For a given spatial discretization it is seen from Fig. 6, that
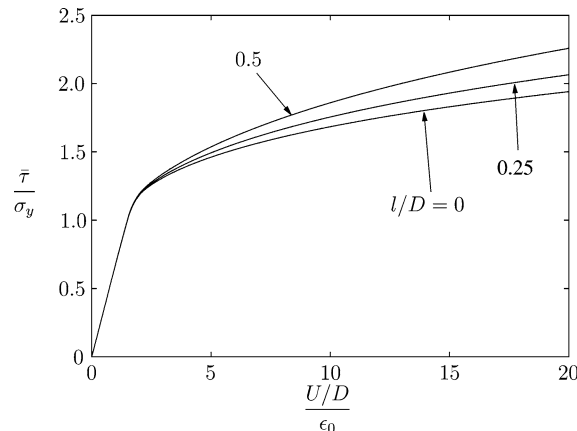


Fig. 5. Average shear stress as a function of the overall deformation, for a rectangular slab of material between rigid platens with $L/D = 1$. The curves show results for different values of the internal material length scale.
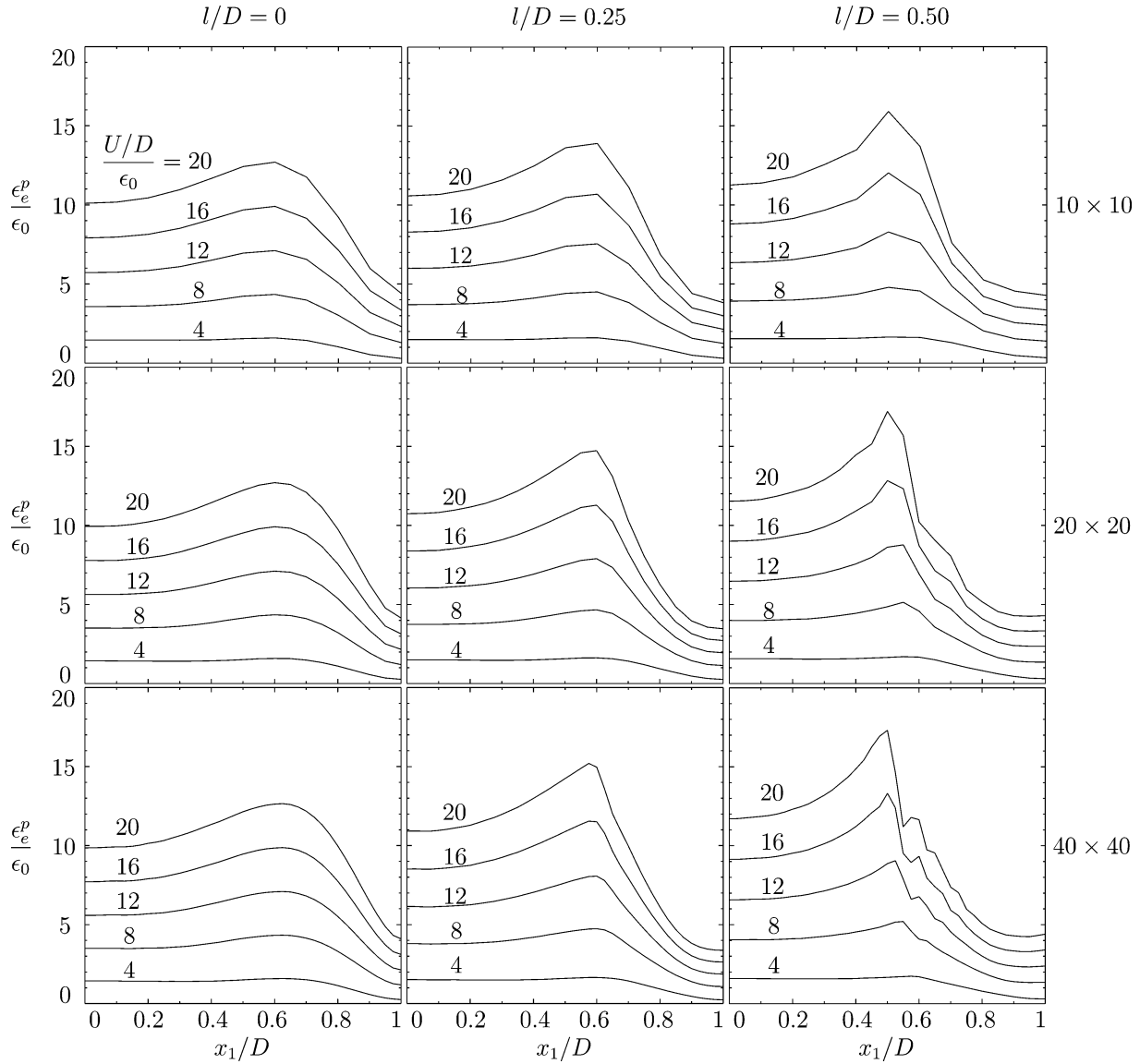
Fig. 6. Plastic strain profiles along the $x_1$-axis for a rectangular slab ($L/D = 1$), at different levels of overall deformation. The figure illustrates how the plastic strain profiles are predicted for different values of the internal material length scale, and for different mesh refinements.

the predicted peak value of effective plastic strain along the $x_1$-axis increases with an increasing internal material length scale. Furthermore, the peak, which remains quite smooth for the conventional solid, becomes more pronounced as the deformation progresses and increasingly narrower the larger $l/D$. It is evident that a vertex in the plastic strain distribution is developing for the solids with $l/D > 0$. The vertex is located along the ridge where the effective plastic strain has a local maximum in the conventional solution. The tangent modulus develops a significant deficit along the ridge for reasons analogous to those discussed in the previous section, leading to the vertex localization. We note in passing that the problem for same geometry and loading but characterized by a higher order strain gradient theory gives rise to smooth distributions of plastic strain (Niordson and Hutchinson, 2003).

The evolution of the effective plastic strain profile is rather insensitive to mesh refinement for the conventional material with $l/D = 0$. By contrast, the peak value of effective plastic strain increases significantly upon mesh refinement when $l/D = 0.25$, and even more so when $l/D = 0.5$. Furthermore, for the most highly refined mesh for $l/D = 0.5$, it is evident that the plastic strain profile becomes increasingly non-smooth with increasing deformation. As the vertex develops, the numerical method has

increasing difficulty rendering an accurate solution. If one were interested in following the development much further than that shown, a method specialized to cope with vertex-like behavior would have to be developed, but that is not our objective.

## 5. Conclusions

Both examples studied here reveal that vertex-type shear localization develops as deformation proceeds in a hardening material characterized by a lower order, strain gradient theory of plasticity. In the infinite layer subject to shear, strain gradients are triggered by an initial non-uniformity, while in the finite layer gradients are present from the start. The vertex distribution of plastic strain is unusual and it is our belief that it is unlikely to have any physical basis. Indeed, in these examples, rather than smoothing the plastic strain distribution as would normally be expected of a strain gradient theory, the lower order gradient theory has the opposite effect. A qualitative explanation of the emergence of vertex localization is given for the infinite layer. The vertex develops at locations where the effective plastic strain is a maximum and its gradients vanish.

Although the two problems investigated here are fairly simple, it is unlikely that they are exceptional as far as the behavior they reveal. The unusual behavior is a consequence of the mathematical formulation of the lower order gradient theories. On the face of it, the modification introduced to create the lower order theory would appear to leave the mathematical character of the field equations unchanged. The order of the field equations for the incremental quantities is the same as for conventional theory. However, the strain gradients introduced into the tangent moduli result in terms in the total (or integrated) quantities appearing in these equations that are more highly differentiated than any that appear in conventional theory. The presence of these terms is directly related to existence of a multiplicity of solutions in problems such as that studied by Volokh and Hutchinson (2002). The present examples provide further evidence that modifying the tangent moduli by a dependence on strain gradients is not necessarily a benign process from a mathematical point of view.

In conclusion, it is worth viewing lower order theories in light of strain gradient elasticity theory, which is a simpler system to envision. If one postulates that the strain energy density of an elastic solid depends on both the strains and gradient of strains, then the resulting theory is inescapably higher order with additional stress quantities and boundary conditions (Mindlin, 1964). The lower order gradient plasticity theory retains the order of conventional theory because only the tangent moduli that appear in the field equations for the incremental quantities are modified using strain gradients in the current state. Additional stress quantities never arise, and, in general, additional boundary conditions for the incremental boundary value problem are neither required nor allowed. The seductive simplicity of this lower order modification strategy would not work for elasticity. Whether it can be justified from a physical standpoint for plasticity remains an open question. The examples presented here indicate that there exist solutions to the lower order formulation that are unexpected and, probably, unphysical.

## References

Acharya, A., Bassani, J.L., 1996. On non-local flow theories that preserve the classical structure of incremental boundary value problems. In: Pineau, A., Zaoui, A. (Eds.), IUTAM Symposium on Micromechanics of Plasticity and Damage of Multiohase Materials. Kluwer Academic, pp. 3–9.

Aifantis, E.C., 1984. On the microstructural origin of certain inelastic models. Trans. ASME J. Engrg. Mat. Tech. 106, 326–330.

Arsenlis, A., Parks, D.M., 1999. Crystallographic aspects of geometrically-necessary and statistically-stored dislocation density. Acta Mater. 47, 1597–1611.

Bassani, J.L., 2001. Incompatibility and a simple gradient theory of plasticity. J. Mech. Phys. Solids 49, 1983–1996.

Bittencourt, E., Needleman, A., Gurtin, M.E., Van der Giessen, E., 2003. A comparison of nonlocal continuum and discrete dislocation plasticity predictions. J. Mech. Phys. Solids 51, 283–310.

Busso, E.P., Meissonneir, F.T., O'Dowd, N.P., 2000. Gradient-dependent deformation of twophase single crystals. J. Mech. Phys. Solids 48, 2333–2362.

de Borst, R., Mühlhaus, H.-B., 1992. Gradient-dependent plasticity: Formulation and algorithmic aspects. Int. J. Numer. Methods Engrg. 35, 521–539.

Fleck, N.A., Hutchinson, J.W., 2001. A reformulation of strain gradient plasticity. J. Mech. Phys. Solids, 2245–2271.

Gao, H., Huang, Y., Nix, W.D., Hutchinson, J.W., 1999. Mechanism-based strain gradient plasticity – I. Theory. J. Mech. Phys. Solids 47, 1239–1263.

Gurtin, M.E., 2000. On the plasticity of single crystals: free energy, microforces plastic-strain gradients. J. Mech. Phys. Solids 48, 989–1036.

Jirasek, M., Bazant, Z.P., 2002. Inelastic Analysis of Structures. Wiley, UK.

Mindlin, R.D., 1964. Micro-structure in linear elasticity. Arch. Rational Mech. Anal. 16, 51–78.

Niordson, C.F., Hutchinson, J.W., 2003. Non-uniform plastic deformation of micron scale objects. Int. J. Numer. Methods Engrg. 56, 961–975.

Volokh, K.Yu., Hutchinson, J.W., 2002. Are lower-order gradient theories of plasticity really lower order?. J. Appl. Mech. 69, 862–864.